Cell Reports Medicine, Volume *5*

Supplemental information

Dietary vitamin B3 supplementation induces the antitumor immunity against liver cancer via biased GPR109A signaling in myeloid cell

Yang Yang, Tianduo Pei, Xiaolin Hu, Yu Lu, Yanqiu Huang, Tingya Wan, Chaobao Liu, Fengqian Chen, Bao Guo, Yuemei Hong, Qian Ba, Xiaoguang Li, and Hui Wang

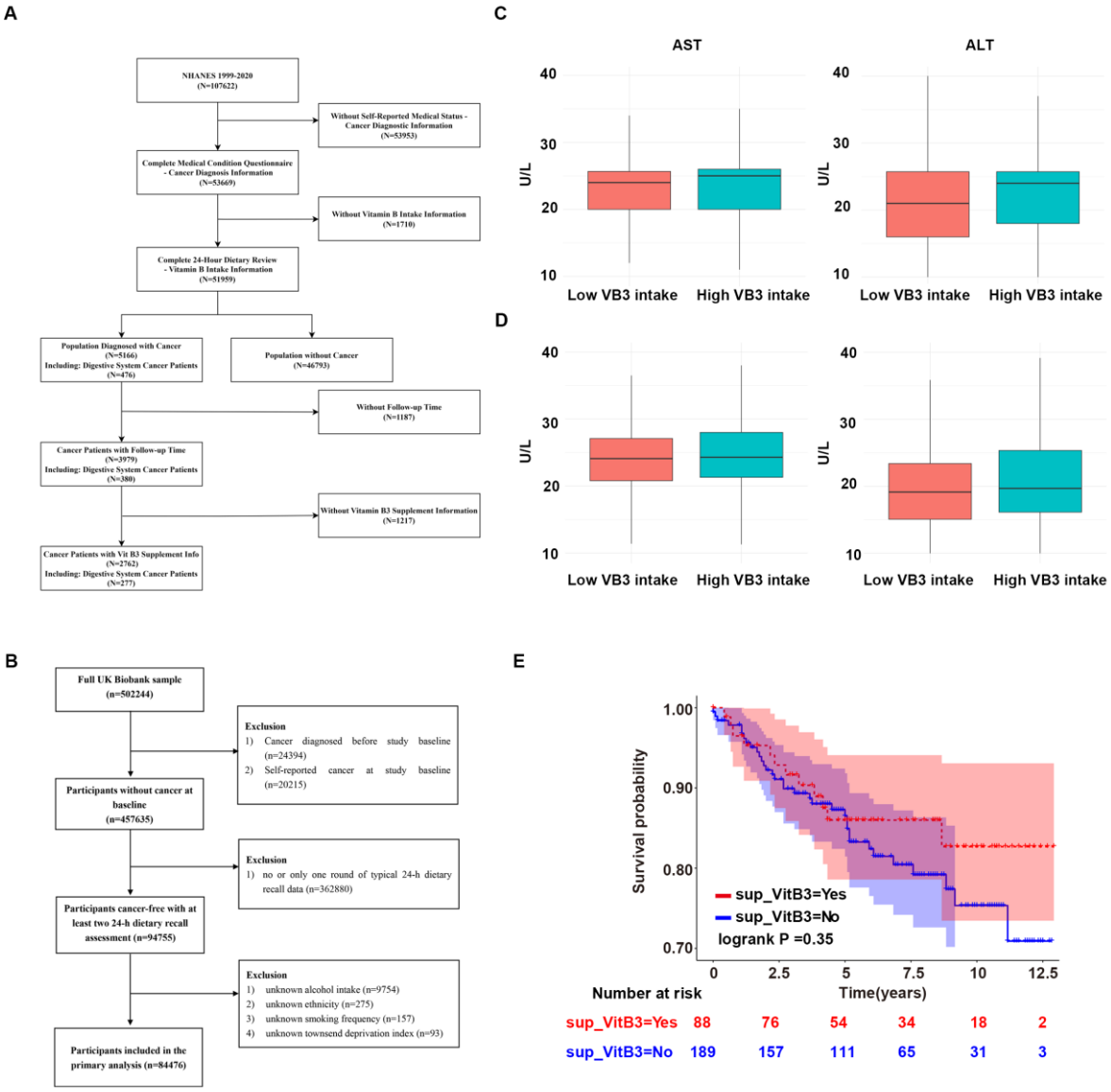

Figure S1. Higher intake of VB3 reduces the risk of liver cancer incidence, related to Figure 1.

(A) Flowchart of population study selection process for NHANES database.

(B) Flowchart of population study selection process for UK Biobank database.

(C) The serum AST and ALT levels of included participants from NHANES database.

(D) The serum AST and ALT levels of included participants from UK Biobank database.

(E) Kaplan-Meier survival curves for VB3 supplementation with digestive system cancers-related mortality outcomes in NHANES database.

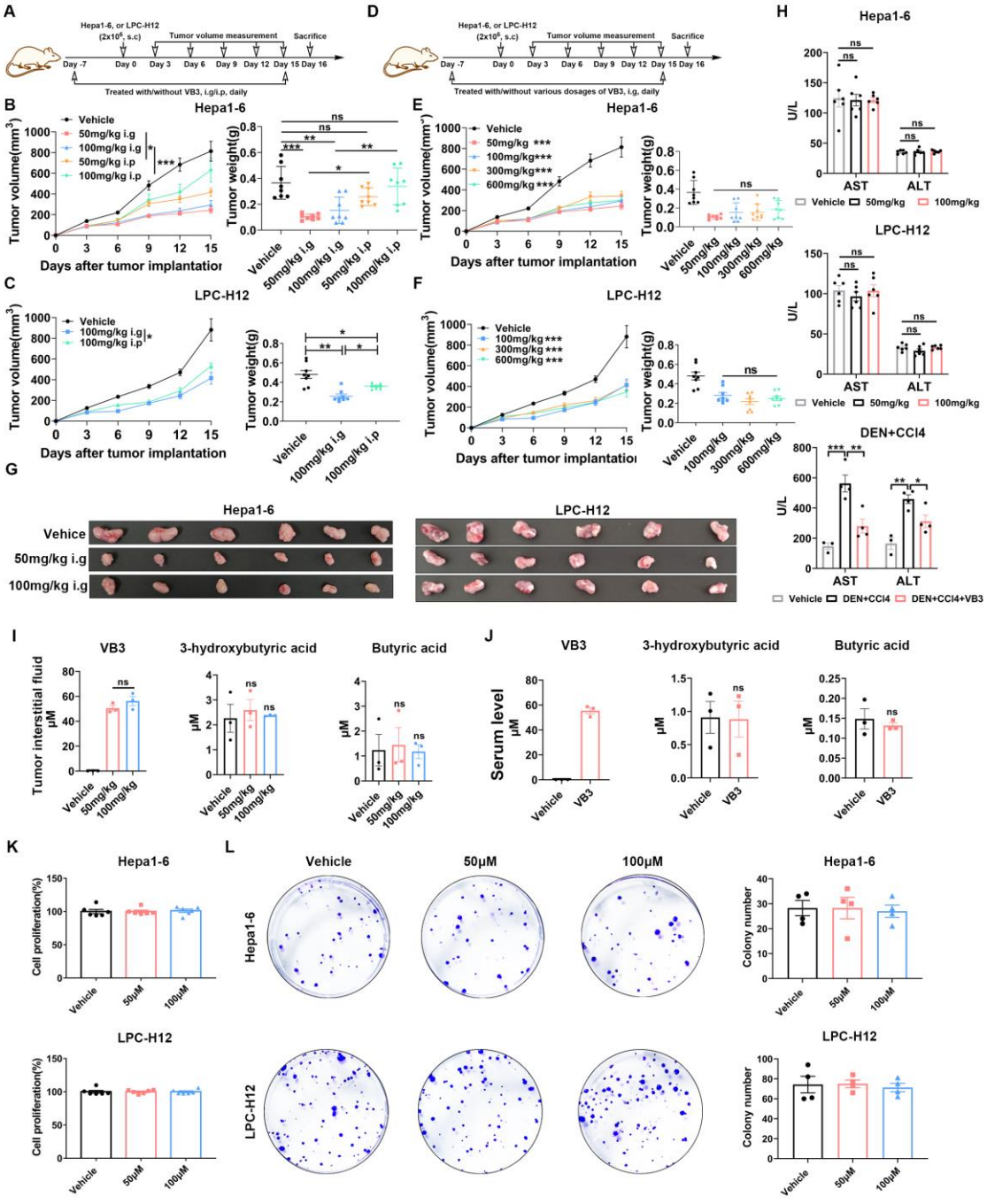

Figure S2. Dietary VB3 supplementation suppresses liver cancer growth, related to Figure 2 and 3.

(A-C) The schedule of establishing subcutaneous liver cancer models and VB3 treatment (A). Tumor volumes and tumor weights of Hepa1-6 (B, n=8) and LPC-H12 (C, n=8) were measured after daily dietary VB3 supplementation (50 or 100mg/kg, i.g or i.p).

(D-F) The schedule of establishing subcutaneous liver cancer models and dietary VB3 supplementation

(D). Tumor volumes and tumor weights of Hepa1-6 (E, n=8) and LPC-H12 (F, n=8) were measured after different dosages VB3 treatment daily (50, 100, 300, and 600mg/kg, i.g).

(G) Representative tumor photos of subcutaneous Hepa1-6 or LPC-H12 tumor model after dietary VB3 supplementation.

(H) The serum AST and ALT levels of VB-treated mice in Hepa1-6, LPC-H12, and DEN+CCl4 models.

(I and J) The contents of VB3, 3-hydroxybutyric acid and butyric acid in the tumor interstitial fluid (I) or serum (J) were determined by LC-MS from Hepa1-6 tumor-burdened mice after VB3 supplementation (n=3).

(K) Hepa1-6 and LPC-H12 tumor cells were treated with VB3 (50μM or 100μM) for 72h, the proliferation rates of VB3-treated cells were assessed by CCK-8 (n=6).

(L) Hepa1-6 or LPC-H12 tumor cells were placed in six-well plates and treated with 50 or 100μM VB3. After 14 days, tumor cells were fixed and tinted. Cell colonies numbers were counted by Image J (n=4).

Data are presented as means ± SEM. Statistical analysis was performed by two-way ANOVA (B, C, E, and F), one-way ANOVA (B, C, E, F, H, I, K, and L) or Student's t test (J). ns, $P>0.05$; *, $P<0.05$; **, $P<0.01$; ***, $P<0.001$.

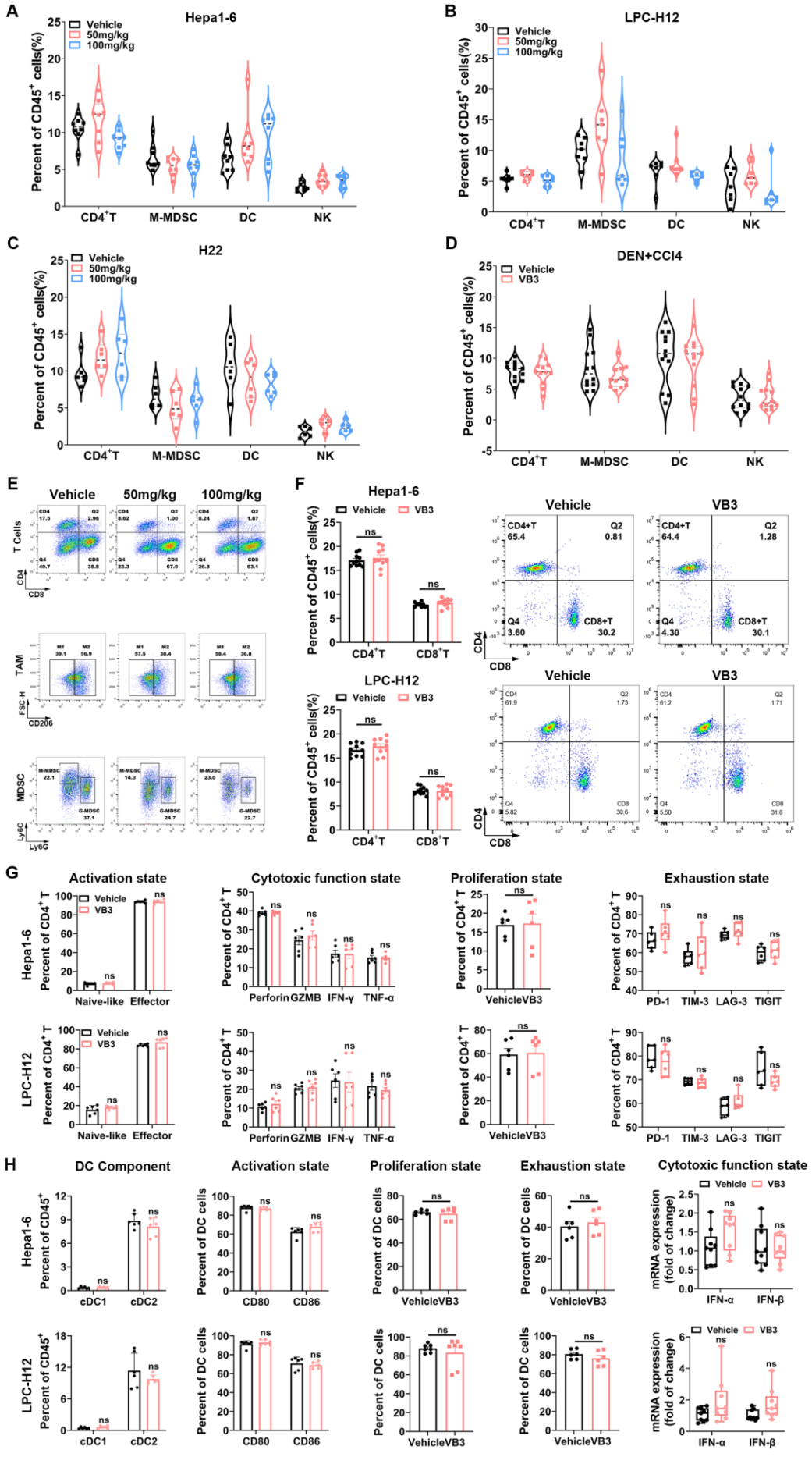
A
Hepa1-6
Vehicle
50mg/kg
100mg/kg
Percent of CD45+ cells(%)
CD4+T
M-MDSC
DC
NK
B
LPC-H12
C
H22
D
DEN+CCl4
Vehicle
VB3
E
Vehicle
50mg/kg
100mg/kg
T Cells
TAM
MDSC
F
Hepa1-6
LPC-H12
CD4+T
CD8+T
G
Activation state
Cytotoxic function state
Proliferation state
Exhaustion state
Naive-like
Effector
Perforin
GZMB
IFN-γ
TNF-α
PD-1
TIM-3
LAG-3
TIGIT
H
DC Component
cDC1
cDC2
CD80
CD86
mRNA expression (fold of change)
IFN-α
IFN-β
ns

Figure S3. The frequency of other infiltrated immune cells in tumor microenvironment, related to Figure 3.

(A-D) The infiltration of $CD4^+$ T cells, M-MDSCs, DCs, and NK cells in tumor microenvironment were analyzed by flow cytometry from tumor tissues in Hepa1-6 (A, n=8), LPC-H12 (B, n=7), H22 (C, n=6), and DEN+CCl4-induced tumor model (D, n=12) after dietary VB3 supplementation.

(E) Representative flow cytometry gating images showed the percentages of $CD4^+$ T cells, $CD8^+$ T cells, M1-like TAMs, M2-like TAMs, M-MDSCs, and G-MDSCs in subcutaneous LPC-H12 model.

(F) The proportion of $CD4^+$ T cells and $CD8^+$ T cells in spleen from tumor-planted mice were determined by flow cytometry after VB3 supplementation (50mg/kg, i.g, n=6).

(G) VB3 supplementation-induced changes in tumor-infiltrated $CD4^+$ T cells from Hepa1-6 and LPC-H12 tumors were determined by flow cytometry (n=6), including activation state (naïve-like $CD4^+$ T, $CD4^+CD44^-CD62L^+$; effector $CD4^+$ T, $CD4^+CD44^+CD62L^-$), cytotoxic function state (Perforin, GZMB, IFN-γ and TNF-α), proliferation state (Ki-67), and exhaustion state (PD-1, TIM-3, LAG-3, and TIGIT).

(H) VB3 supplementation-induced changes in tumor-infiltrated DCs from Hepa1-6 and LPC-H12 tumors were determined by flow cytometry (n=6), including component (cDC1, $XCR1^+CD172^-$; cDC2, $XCR1^-CD172^+$), activation state (CD80 and CD86), proliferation state (Ki-67), and exhaustion state (PD-L1). The cytotoxic function state of sorted DCs in tumor microenvironment after VB3 intervention were determined by RT-qPCR, including IFN-α and IFN-β.

Data are presented as means ± SEM. Statistical analysis was performed by one-way ANOVA (A, B, and C) or Student's t test (D, F, G, and H). ns, $P>0.05$; *, $P<0.05$; **, $P<0.01$; ***, $P<0.001$.

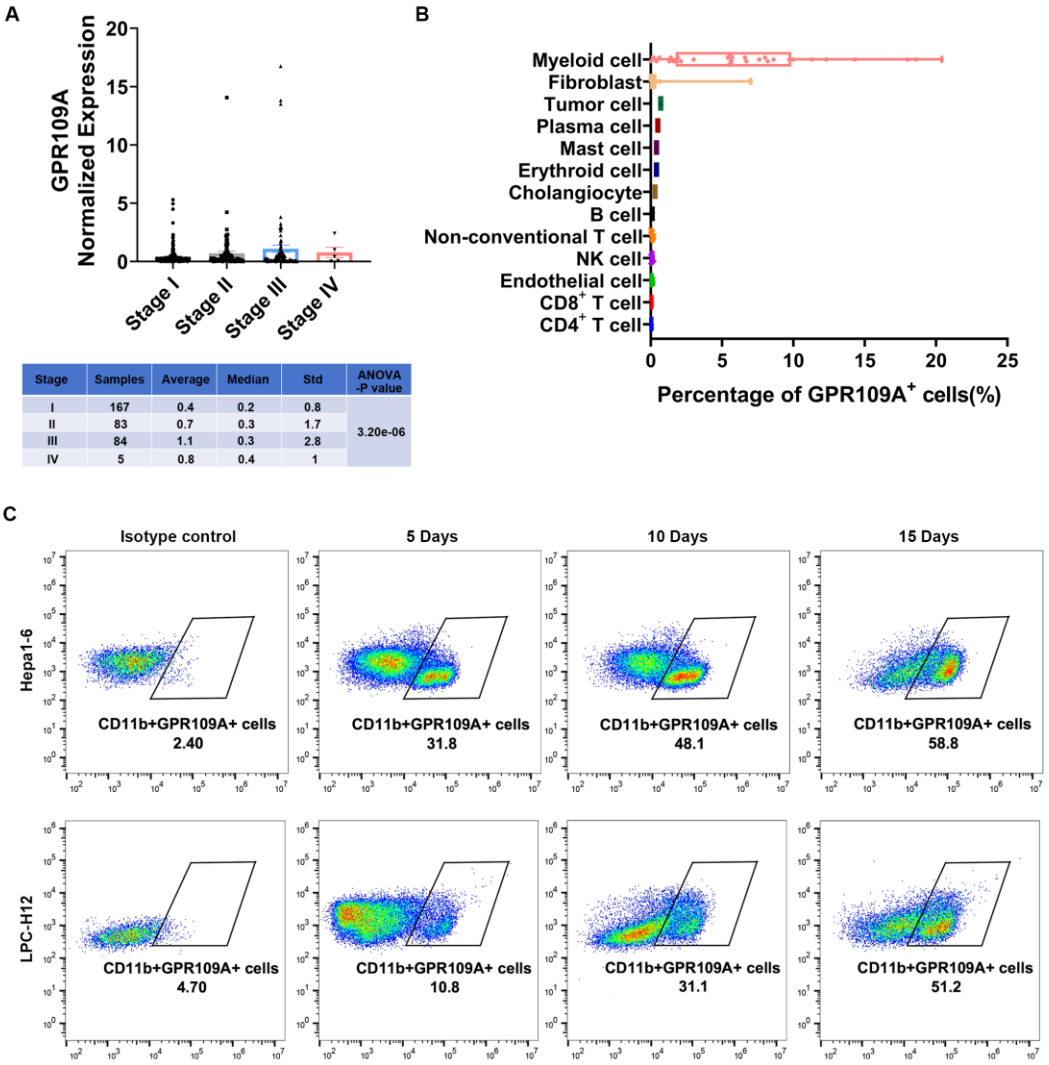

Stage	Samples	Average	Median	Std	ANOVA -P value
I	167	0.4	0.2	0.8	3.20e-06
II	83	0.7	0.3	1.7	
III	84	1.1	0.3	2.8	
IV	5	0.8	0.4	1	

Figure S4. The expression atlas and dynamic changes of GPR109A in liver cancer tumor microenvironment, related to Figure 5.

(A) The GPR109A mRNA expression difference in various stages of liver cancer patients.

(B) The GPR109A mRNA expression atlas of different cells subtypes in tumor microenvironment was plotted by processed single-cell RNA-seq data from liver cancer patients.

(C) Representative flow cytometry gating images showed the percentages of GPR109A expression on tumor-infiltrated myeloid cells at day 5, day 10, and day 15 after Hepa1-6 and LPC-H12 tumor implantation.

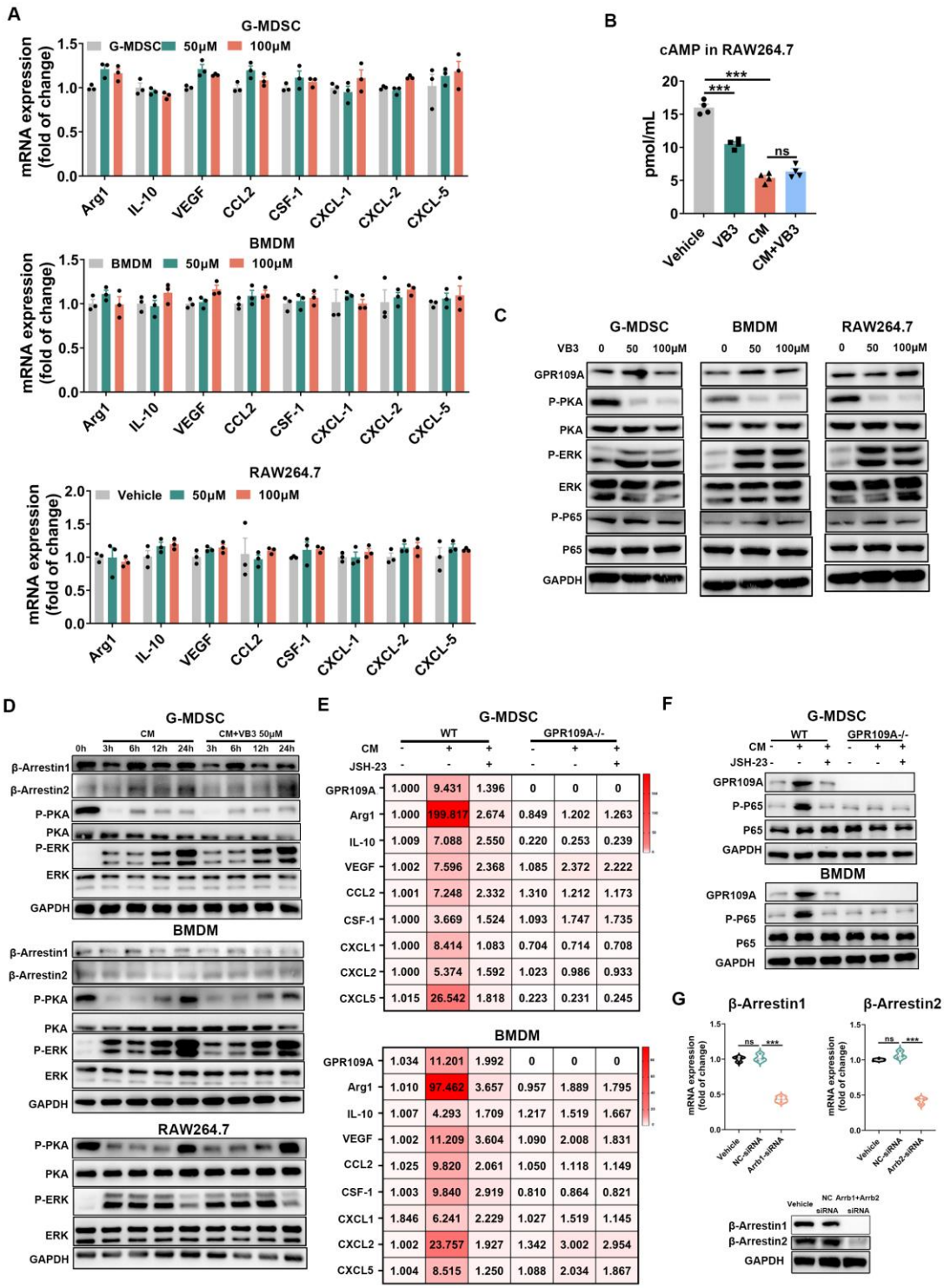

Figure S5. The influence of VB3 treatment on normal and CM-treated myeloid cells, related to Figure 6.

(A) Primary G-MDSC and BMDM from C57BL/6 mice or RAW264.7 cell line were treated with VB3 (50 or 100μM) for 12h. The mRNA expression of GPR109A, Arg-1, IL-10, VEGF, CCL2, CSF-1,

CXCL1, CXCL2, and CXCL5 were detected by RT-qPCR (n=3).

(B) RAW264.7 cells were treated with/without LPC-H12 CM and 50μM VB3 for 12h. The intracellular cAMP level was detected by ELISA assay (n=4).

(C) Primary G-MDSC and BMDM from C57BL/6 mice or RAW264.7 cell line were treated with VB3 (50 or 100μM) for 12h. The protein expression of GPR109A, P-PKA, PKA, P-ERK, ERK, P-P65, and P65 in each group was quantified by western blotting.

(D) Primary G-MDSC and BMDM from wild type C57BL/6 mice or RAW264.7 cell line were treated with LPC-H12 CM and 50μM VB3 for different time intervals (0, 3, 6, 12, and 24h). The protein expression of β-Arrestin1, β-Arrestin2, P-PKA, PKA, P-ERK, and ERK in each group was determined by western blotting.

(E and F) Primary G-MDSC and BMDM from wild type or GPR109A-/- C57BL/6 mice were treated with/without LPC-H12 CM and JSH-23 (10μM) for 12h. The mRNA expression of GPR109A, Arg-1, IL-10, VEGF, CCL2, CSF-1, CXCL1, CXCL2, and CXCL5 were detected by using RT-qPCR (E). The protein expression of GPR109A, P-P65, and P65 were explored by western blotting (F).

(G) The knockdown efficacy of β-Arrestin1/2 siRNA was evaluated by RT-qPCR and western blotting. Data are presented as means ± SEM. Statistical analysis was performed by one-way ANOVA (A, B, and G). ns, $P>0.05$; *, $P<0.05$; **, $P<0.01$; ***, $P<0.001$.

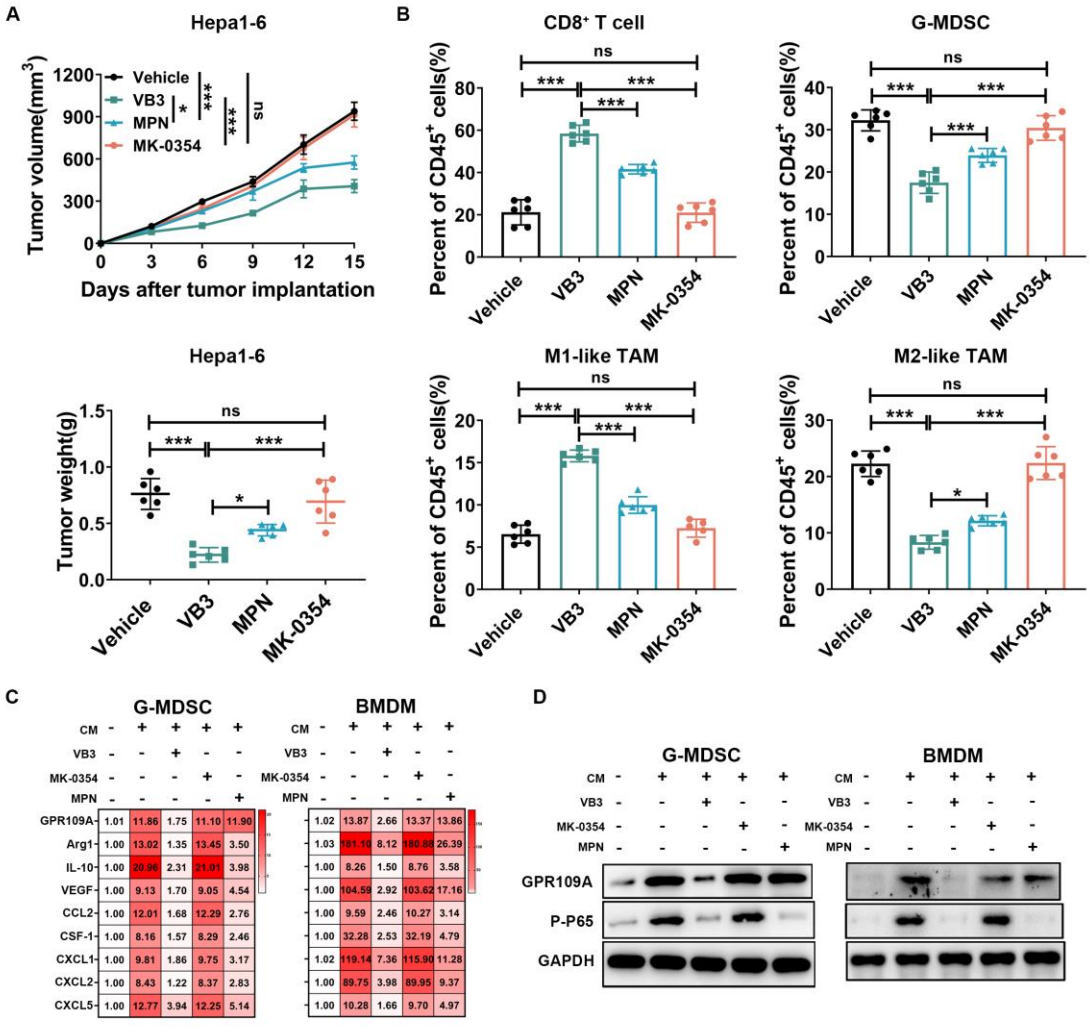

Figure S6. The anti-tumor effect of VB3, MPN, and MK-0354 against liver cancer, related to Figure 6.

(A and B) C57BL/6 mice were pretreated with daily intake of VB3 (50mg/kg, i.g), MPN (50mg/kg, i.p), MK-0354 (50mg/kg, i.p) for 7 days. Then, 2 x 10^6 Hepa1-6 tumor cells were subcutaneously injected into mice. Tumor volumes and tumor weights were measured after daily indicated treatment (A, n=6). The frequency of $CD8^+$ T cells, G-MDSCs, M1-TAMs, and M2-TAMs in tumor microenvironment were analyzed by flow cytometry (B, n=6).

(C and D) Primary G-MDSC and BMDM from wild type C57BL/6 mice were treated with Hepa1-6 CM, VB3 (50μM) MK-0354 (50μM), or MPN (50μM) for 12h. The mRNA expression of GPR109A,

Arg-1, IL-10, VEGF, CCL2, CSF-1, CXCL1, CXCL2, and CXCL5 were detected by using RT-qPCR (C). The protein expression of GPR109A and P-P65 were detected by western blotting (D).

Data are presented as means ± SEM. Statistical analysis was performed by two-way ANOVA (A) and one-way ANOVA (A-C). ns, $P>0.05$; *, $P<0.05$; **, $P<0.01$; ***, $P<0.001$.

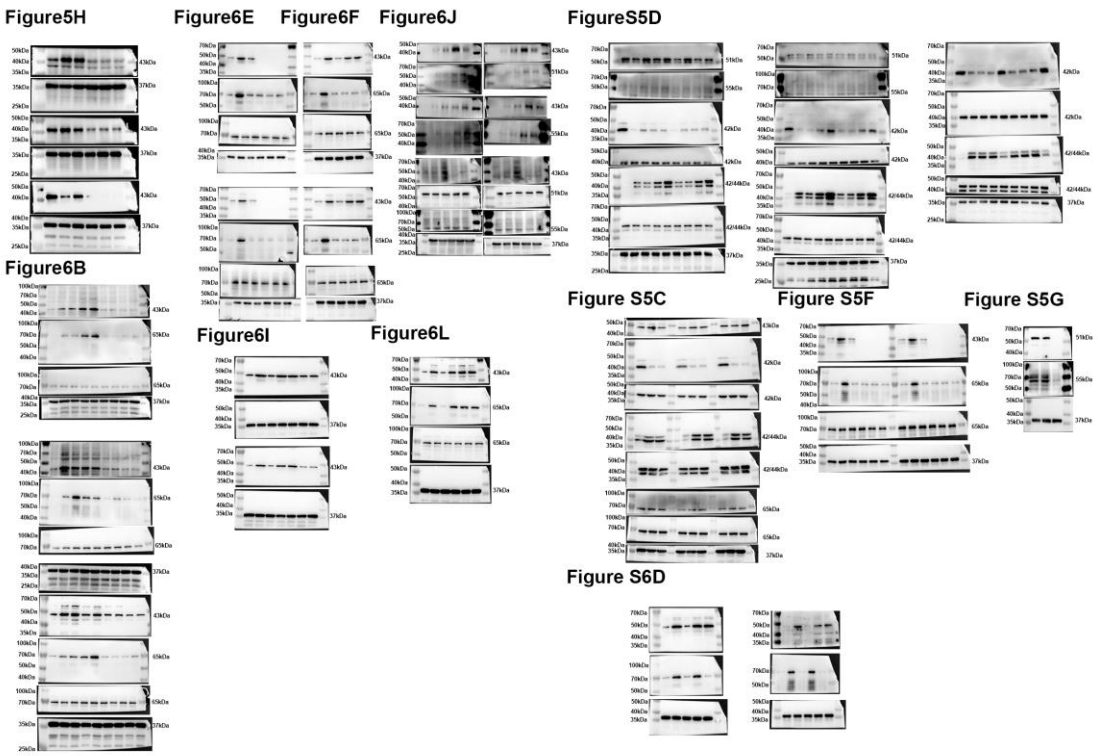

Figure S7. The uncropped membranes of western blot, related to Figure 5, 6 and Figure S5, 6.

Table S1 Demographic baseline characteristics: NHANES (1999 to 2020), related to Figure 1 and Figure S1.

Characteristics	Non-Cancer population (N=46793)	Digestive system Cancer Patients (N=476)	P-value
Age, years, Mean (SD)	47.92(17.66)	69.35(11.95)	<0.01
Gender, n (%)			0.08
Male	22621(48.34)	249(52.31)	
Female	24172(51.66)	227(47.69)	
Ethnicity, n (%)			<0.01
Mexican American	8493(18.15)	35(7.35)	
Other Hispanic	4058(8.67)	28(5.88)	
Non-Hispanic White	19539(41.76)	281(59.03)	
Non-Hispanic Black	10422(22.27)	107(22.48)	
Other Race-Including Multi-Racial	4281(9.15)	25(5.25)	
Marital status, n (%)			<0.01
Married/Living with Partner	23800(50.86)	207(43.49)	
Widowed/Divorced/Separated	15657(33.46)	191(40.13)	
Refused or unknown	7336(15.68)	78(16.39)	
Educational level, n (%)			<0.01
Less than high school	23329(49.86)	277(58.19)	
High school or higher	23409(50.03)	198(41.60)	
Refused or unknown	55(0.12)	1(0.21)	
Family income-to-poverty ratio, n (%)			0.06
≤1.30	13350(28.24)	144(30.25)	
1.30-3.50	16137(34.49)	181(38.03)	
>3.50	13184(28.18)	108(22.69)	
Refused or unknown	4122(8.81)	43(9.03)	
Vitamin B intake, grams, Mean (SD)			
Vitamin B1	1.58(0.82)	1.50(0.87)	0.05
Vitamin B2	2.02(1.14)	1.95(1.16)	0.16
Vitamin B3	24.33(13.31)	21.49(11.64)	<0.01
Vitamin B6	1.99(1.32)	1.84(1.20)	0.01
Vitamin B12	5.01(6.60)	4.84(5.61)	0.57

Descriptive data were shown as mean (SD) while categorical variables were reported as n (%). P-values less than 0.05 ($p < 0.05$) were considered significant. n: number.

Table S2 Baseline characteristics of 84,476 participants by median of vitamin B3 intake in the UK Biobank, related to Figure 1 and Figure S1.

Characteristics	Overall	Vitamin B3 intake≤ 37.50mg/d	Vitamin B3 intake> 37.50 mg/d	P-value
Sample size (N)	84476	42239	42237	
Age, years (median [IQR])	57.00 [50.00, 62.00]	57.00 [50.00, 62.00]	57.00 [50.00, 63.00]	0.900
Gender (%)				
female	44816 (53.1)	27006 (63.9)	17810 (42.2)	<0.001
male	39660 (46.9)	15233 (36.1)	24427 (57.8)	
Ethnicity (%)				
Asian or Asian British	1065 (1.3)	671 (1.6)	394 (0.9)	<0.001
Black or Black British	677 (0.8)	324 (0.8)	353 (0.8)	
Other ethnic groups	914 (1.1)	468 (1.1)	446 (1.1)	
White	81820 (96.9)	40776 (96.5)	41044 (97.2)	
Education qualification (%)				
College or university degree/vocational qualification	61847 (73.2)	30059 (71.2)	31788 (75.3)	<0.001
National examination at age 16	11575 (13.7)	6274 (14.9)	5301 (12.6)	
National examination at age 17-18	5249 (6.2)	2723 (6.4)	2526 (6.0)	
Unknown	5805 (6.9)	3183 (7.5)	2622 (6.2)	
Townsend deprivation index (%)				
Least deprived, –6.26- –3.32	28222 (33.4)	13639 (32.3)	14583 (34.5)	<0.001
Intermediate, –3.31- –1.09	28130 (33.3)	13975 (33.1)	14155 (33.5)	
Most deprived, –1.08-10.27	28124 (33.3)	14625 (34.6)	13499 (32.0)	
BMI, kg/m^2 (median [IQR])	25.90 [23.50, 28.89]	25.65 [23.24, 28.63]	26.16 [23.78, 29.13]	<0.001
Alcohol intake, g/d (median [IQR])	12.93 [5.38, 23.84]	11.46 [4.20, 21.48]	14.54 [6.64, 26.52]	<0.001
Cigarette smoking status (%)				
Current	5716 (6.8)	2874 (6.8)	2842 (6.7)	0.034
Never	48086 (56.9)	24209 (57.3)	23877 (56.5)	
Previous	30674 (36.3)	15156 (35.9)	15518 (36.7)	

Table S3. Primer sequences used for RT-PCR in study, related to the STAR Methods.

REAGENT or RESOURCE	SOURCE	IDENTIFIER
Mouse GPR109A Forward: CTGGAGGTTCGGAGGCATC Reverse: TCGCCATTTTTGGTCATCATGT	This paper	N/A
Mouse Arg-1 Forward: ACCTGGCCTTTGTTGATGTCCCTA Reverse: AGAGATGCTTCCAACTGCCAGACT	This paper	N/A
Mouse IL-10 Forward: TGCACTACCAAAGCCACAAGGCAG Reverse: AGTAAGAGCAGGCAGCATAGCAGT	This paper	N/A
Mouse VEGF Forward: GCACATAGAGAGAATGAGCTTCC Reverse: CTCCGCTCTGAACAAGGCT	This paper	N/A
Mouse CCL2 Forward: TTAAAAACCTGGATCGGAACCAA Reverse: GCATTAGCTTCAGATTTACGGGT	This paper	N/A
Mouse CSF-1 Forward: GGCTTGGCTTGGGATGATTCT Reverse: GAGGGTCTGGCAGGTACTC	This paper	N/A
Mouse CXCL1 Forward: CTGGGATTCACCTCAAGAACATC Reverse: CAGGGTCAAGGCAAGCCTC	This paper	N/A
Mouse CXCL2 Forward: CAGAAGTCATAGCCACTCTCAAG Reverse: CTCCTTTCCAGGTCAGTTAGC	This paper	N/A
Mouse CXCL5 Forward: TCGCTAATTTGGAGGTGATCC Reverse: TTGTCACTGCCCAATATTTTCTG	This paper	N/A
Mouse β-actin Forward: AGAGGGAAATCGTGCGTGAC Reverse: CAATAGTGATGACCTGGCCGT	This paper	N/A
Mouse CD163 Forward: ATGGGTGGACACAGAATGGTT Reverse: CAGGAGCGTTAGTGACAGCAG	This paper	N/A
Mouse IFN-α Forward: TGTCTGATGCAGCAGGTGG Reverse: AAGACAGGGCTCTCCAGAC	This paper	N/A
Mouse IFN-β Forward: AGCTCCAAGAAAGGACGAACA Reverse: GCCCTGTAGGTGAGGTTGAT	This paper	N/A